Reduced mobility and rate coefficients for H_2^+ ions in H_2 gas

Ž.D. Nikitović and Z.M. Raspopović

Institute of Physics Belgrade, University of Belgrade,
Pregrevica 118, 11080 Belgrade, Serbia

Abstract. In this work, we present a complete cross sections set that describe the interaction between H_2^+ ions and H_2 molecules. Based on these cross sections, we have calculated the transport properties of H_2^+ ions in H_2 gas, depending on the reduced electric field. Ionic charge exchange reactions with molecules are indispensable elementary processes in the modeling of kinetics in terrestrial, industrial and astrophysical plasma in the detection of dark matter. A Monte Carlo simulation method is applied to accurately calculate transport parameters in hydrodynamic regime. We discuss new data for H_2^+ ions in H_2 gas where the mean energy the flux and bulk values of reduced mobility and other transport coefficients, are given as a function of low and moderate reduced electric fields.

Key words: H_2^+ ions – H_2 gas – Monte Carlo simulation – cross sections – transport parameters

1. Introduction

Transport properties of species in gas plasmas are of great importance in understanding the nature of molecular and ionic interactions in gas mixtures (Todd *et al.*, 2002; Mason, 1957; Golzar *et al.*, 2014). These properties include the mean energy, drift velocity, diffusion coefficients, ionization and chemical reaction coefficients, chemical reaction coefficients for ions and (rarely) excitation coefficients, and they are very useful in chemical industries for the design of many types of transport and process equipment.

H_2 gas is used in gaseous electronic multipliers for various imaging purposes (X-rays, charged particles, thermal neutrons and dark matter detection) (Fraga *et al.*, 2003; Kaboth *et al.* 2008). Hydrogen, is one of the most common elements on Earth and in its gaseous form is a fuel for obtaining energy. Hydrogen is a highly explosive gas and creates one of the highest flame temperatures.

We acknowledge the importance of the results obtained, which provide atomic and molecular data regarding ion transport properties in gases, depending on the reduced electric field, *E/N* (*E*-electric field, *N*-gas density). These data as essential input parameters for modeling various environments. Low temperature

can change the state of metals, gases, liquids and solids, cause damage to organisms depending on length of exposure, and change the functionality of mechanized processes. Quantum-mechanical calculation of a certain cross-section is a required task that requires knowledge of the surface potential energy of ions and molecules to be constructed from the structure of the reactants. Less intensive computational methods, such as the Denpoh-Nanbu theory (Denpoh & Nanbu, 1998; Nikitović *et al.* 2014; Petrović *et al.*, 2007), require knowledge of thermodynamic formation data and are applicable to a range of molecules.

Charge exchange reactions between molecular ions and the parent gas are important elementary processes in modeling kinetics in all types of plasma. In many cases, the cross section for these reactions is known to be the most significant part of the set. The cross-section set describes the total collision cross-section between an ion and a gas particle. The total collision cross-section between an ion and a gas particle is described at low energies using Langevin's cross-section and at higher energies using the collision of rigid spheres, as demonstrated in paper (Nikitović *et al.*, 2016; Nikitović *et al.*, 2019).

Transport parameters of H_2^+ ions in H_2 gas, such as ion energy probability functions, mean energy, drift velocity, reduced mobility, longitudinal and transverse diffusion coefficients, and rate coefficients, are calculated using Monte Carlo simulation. Calculated flux and bulk reduced mobilities exhibit significant differences in the region of moderate *E/N*. The novelty of the work is the first-ever detailed presentation of a set of cross-sections for the interaction of H_2^+ ions with an H_2 molecule, as well as the results of transport coefficients of H_2^+ ions in an H_2 gas.

2. Cross section sets

Transport properties needed for modeling H_2 discharges containing H_2^+ ions are calculated by the Monte Carlo method. A code that properly takes into account thermal collisions was used (Ristivojević & Petrović, 2012). For collisions of H_2^+ ions with H_2 molecules, at energies below 1 eV, the total cross-section is labeled as 'Langevin' in Figure 1 and includes anisotropic forward scatterings, an isotropic capture part, rotational excitations, as well as the charge exchange reaction. The transition from Langevin's cross-section to the collision of rigid spheres (labeled as σ HS in the figure) occurs at energies around 1 eV.

At low collision energies, below 1 eV, predominantly influenced by the induced dipole interaction between ions and molecules, an exothermic proton transfer reaction prevails. As energy increases, H_2^+ ions cease to be effectively captured by the induced dipole forces of H_2 molecules, leading to a observed cross-section displaying a $1/v^3$ trend (Krstić *et al.*, 2009), where v signifies the center-of-mass velocity. Beyond 1 eV, the cross-section for elastic momentum transfer corresponds to direct collisions involving rigid spheres. Initially, collisions of these rigid spheres at low energies may be perceived as isotropic. How-
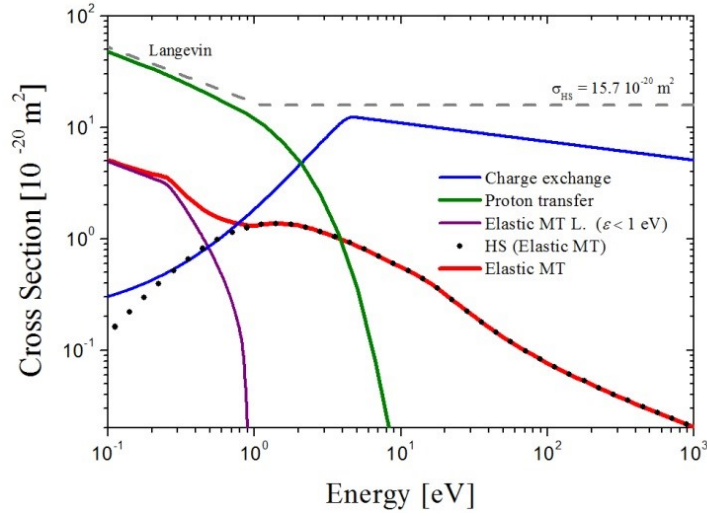
Figure 1. Elastic momentum transfer cross section for collisions between H_2^+ ions and H_2 molecules as a function of collision energy.
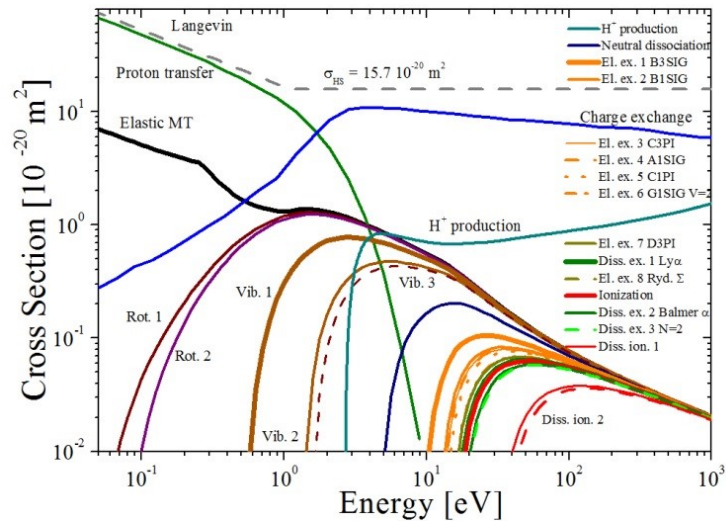

Figure 2. Complete set of cross sections for ion (H_2^+) and molecule (H_2) interactions as a function of collision energy.

ever, with escalating collision energy, their isotropic nature diminishes, progressively favoring forward-directed collisions. Consequently, the momentum transfer cross-section for rigid spheres diminishes with increasing collision energy.
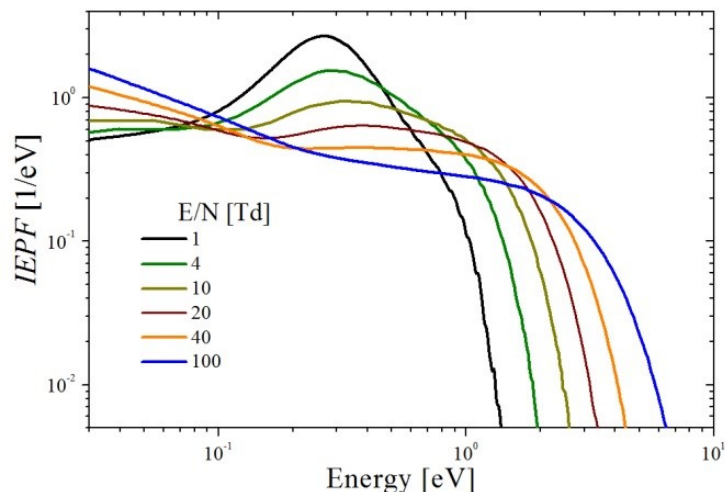

Figure 3. Ion energy probability functions from E/N = 1 Td to E/N = 100 Td.

This decrease is indicated by the black circles in Figure 1 and labeled as "HS (Elastic MT)," as proposed by Denpoh and Nanbu theory (Denpoh & Nanbu, 2022), relative to the total cross section of rigid spheres σ_{HS}. The elastic momentum transfer cross section used in the simulations presented in this study, labeled as 'Elastic MT' in the legend of Figure 1, is a superposition of two cross sections. The first one dominates at low energies and is caused by the induced dipole force between H_2^+ ions and H_2 molecules, denoted as 'Elastic MT L' in the legend. The second cross section results from their direct collision as rigid spheres and is labeled as 'HS (Elastic MT)' in the legend.

At low energies, the primary interaction between ions and gas particles is the induced dipole force, which depends on the collision energy (ε) and the polarizability (α) of the gas particle. The polarizability of H_2 molecules is assumed to be $\alpha = 0.803$ Å^3 (Radzig & Smirnov, 1986). This interaction gives rise to a momentum transfer cross section for collisions, commonly referred to as the Langevin cross section in the literature. Direct collisions between ions and molecules, ions captured by the induced dipole force of molecules resulting in direct collision, and collisions where ions only change direction due to the proximity of gas molecules are encompassed by the Langevin cross section.

At low energies, the primary exothermic reaction is $H_2^+ + H_2 \rightarrow H_3^+ + H$, which is labeled as "proton transfer" in Figure 1. The cross section for this
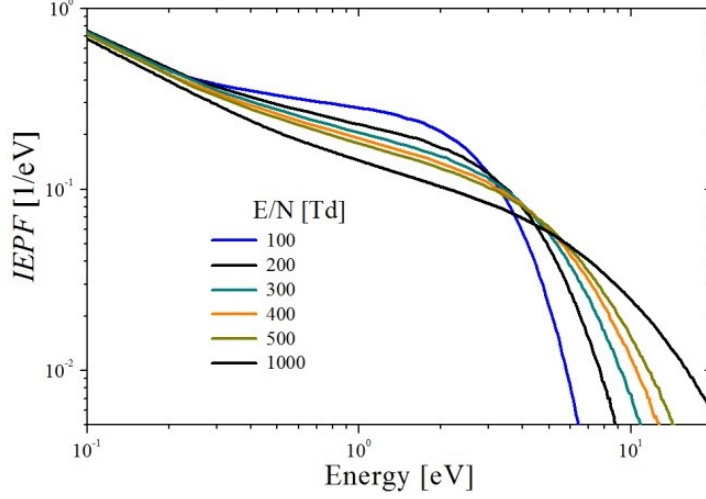
Figure 4. Ion energy probability functions from E/N = 100 Td to E/N = 1000 Td.

reaction is taken from the study by Phelps (1990), but scaled to match that of Denpoh and Nanbu theory (Denpoh & Nanbu, 2022) at an energy of 0.1 eV. The cross section for charge exchange, which refers to the formation of slow H_2^+ as labeled in the legend of Figure 1, was obtained from the study by (Phelps, 1990; Phelps, 2009). At energies below 5 eV, the charge-transfer cross section decreases as a result of competing with the formation of H_3^+.

The elastic momentum transfer cross section used in the simulations presented in this study, labeled as "Elastic MT" in the legend of Figure 1, comprising of two distinct components. Above 1 eV, it is represented by the "HS (Elastic MT)" cross section, while below 1 eV, it is the sum of the "HS (Elastic MT)" and the cross section denoted as "Elastic MT L." in the legend of Figure 1. The elastic momentum transfer cross section at low energies ($\varepsilon < 1$ eV), which originates from the induced dipole interaction (Elastic MT L.), was obtained by subtracting the cross sections of proton transfer, charge exchange reactions, and HS (Elastic MT) from the Langevin cross section. The cross section for this interaction decreases with increasing collision energy, and at 1 eV, it asymptotically approaches zero with a $1/v^3$ dependence.

Figure 2 presents a complete set of cross sections for ion-H_2 molecule interactions as a function of collision energy. The provided cross sections by (Denpoh & Nanbu, 2022) are presented, except for those for proton transfer, H+ production, and charge exchange, for which the cross sections were obtained from Phelps' work (Phelps, 1990; Phelps, 2011). The set includes elastic momentum transfer cross section denoted as "Elastic MT" in Figure 1. The set encompasses rotational ($H_2^+ + H_2$, Rot.), vibrational ($H_2^+ + H_2$, Vib.), electronic ($H_2^+ + H_2$,

El. ex.), and dissociative (H_2^+ + 2H, Diss. ex.) excitations, in addition to Neutral dissociation (H_2^+ + 2H, Neutral dissociation) and Ionization (H_2^+ + H_2^+ + e, Ionization), as well as dissociative ionization (H_2^+ + H^+ + H + e, Diss. Ionization) along with the other mentioned processes. The reaction products of H_2^+ + H_2 shown in parentheses, along with the corresponding labels on the Figure 2.

Non-elastic excitation processes are treated isotropically. In the case of ionization processes, the secondary ion H_2^+ is also tracked, which shares the incoming kinetic energy with the primary ion reduced by the reaction threshold. The partition of kinetic energy between the primary and secondary ions is determined randomly. In the case of proton transfer processes, the resulting ion H_3^+ is not tracked in the simulations, nor is the H^+ ion in the case of H^+ production.
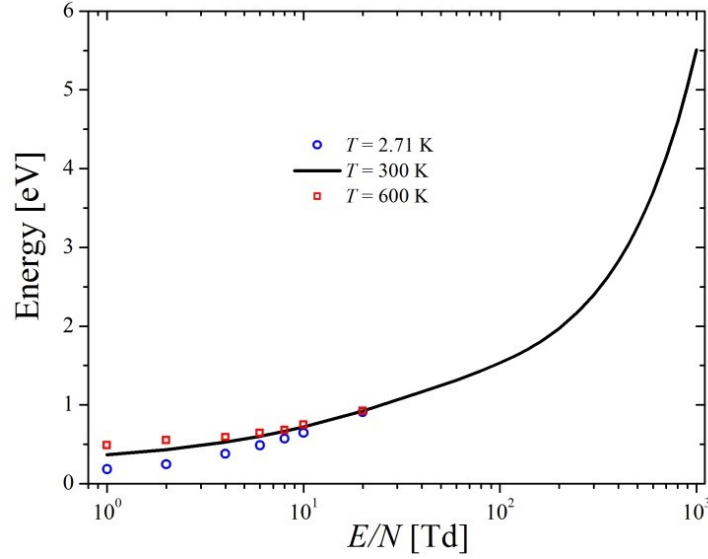

Figure 5. Mean energy of H_2^+ ions a function of E/N.

3. Results and discussion

During the relaxation of H_2^+ ions in H_2 molecules, an energy balance is established between the ion energy gains from the electric field and collisional energy losses. This leads to the appearance of ion energy probability functions (IEPF), as shown in Figure 3 for E/N values between 1 and 100 Td, and in Figure 4 for E/N values between 100 and 1000 Td.

The proton transfer reaction, responsible for the disappearance of H_2^+ ions from the swarm, is highly intense and even occurs at subthermal energies. As a
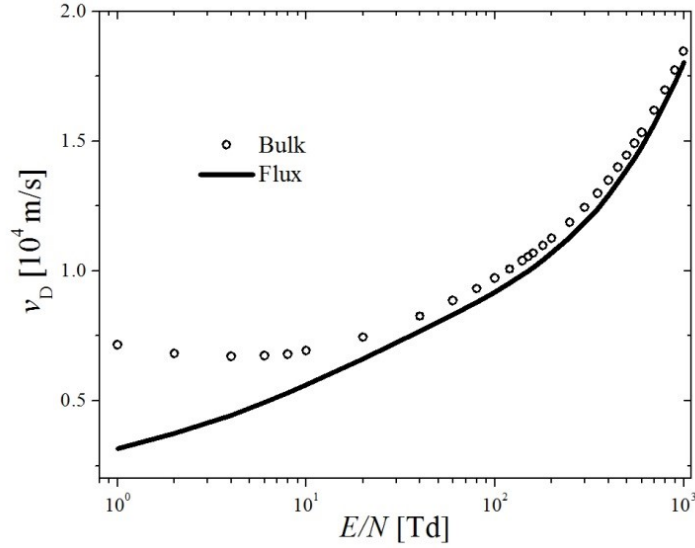
Figure 6. Bulk and flux drift velocity for H_2^+ in H_2 a function of E/N at 300 K.

result, the slow ion population is lacking in the 1-10 Td range, as observed in Figure 3. With increasing electric field intensity, more intense charge exchange reactions take place, leading to the production of slow H_2^+ ions and an increase in the probability of H_2^+ ions being at low energies, as depicted in Figures 3 and 4.

Overall, the ion energy probability function for the H_2^+ and H_2 system significantly deviates from the thermal Maxwell-Boltzmann distribution of ions by energy, for all electric field values.

After reaching steady-state values, the swarm parameters are plotted in Figures 5 to 9 as a function of reduced electric field. Proton transfer reactions deplete the swarm of low-energy H_2^+ ions, resulting in a mean ion energy of 0.37 eV at $E/N = 1$ Td, which is significantly higher than the thermal energy of H_2 molecules at T =300 K. The rise in mean energy is strongly resisted by charge exchange, rotational and vibrational excitation as the electric field increases. With increasing energy, the rate of charge exchange reactions decreases, allowing the mean energy to rise more quickly after E/N > 200 Td. Figure 5 displays not only the mean kinetic energy of ions at a reference temperature of 300 K but also includes data for the mean kinetic energy of ions at gas temperatures of 2.71 K and 600 K. The impact of gas temperatures on the mean kinetic energy of ions becomes noticeable for reduced field strengths below 20 Td.

Figure 6 depicts the drift velocities (Robson *et al.*, 2005; Ness & Robson, 1986; Nikitović *et al.*, 2018; Nikitović & Raspopović, 2021) obtained by simula-

tions using the Monte Carlo method in both real space (bulk) and velocity space (flux). Bulk values are computed as the center of mass displacement over time, $\Delta z_{c.m}/\Delta t$, while flux values correspond to the mean velocity of ions, $<v>$. Non-conservative processes are responsible for separating the bulk and flux values from the transport parameters. The reason for the significantly higher bulk drift velocity values compared to flux drift velocity values in Figure 6 is the decrease in the cross-section for proton transfer interactions with increasing energy. This leads to a greater depletion of H_2^+ ions from the swarm with energies lower than the mean energy value compared to those with higher energies. While the flux drift velocity increases, the slight decrease in bulk drift velocity observed as E/N increases from 1 to 10 Td indicates a reduction in the center of mass displacement over time as the electric field intensity increases. This reduction is due to the interplay between proton transfer reactions, in which slow H_2^+ ions predominantly disappear, and an increase in slow H_2^+ ions resulting from charge exchange reactions.

As a result, at reduced electric fields where ion energies reach the threshold for reaction and H^+ production, the disappearance of high-energy ions from the swarm begins. This results in decreasing differences between bulk and flux drift velocities with increasing E/N. When transitioning from Langevin's cross-section to the collision of rigid spheres, a significant decrease in the elastic momentum transfer cross-section is commonly observed, leading to the appearance of a maximum in the reduced mobility as a function of E/N (Nikitović *et al.*, 2016). In the case of the observed H_2^+ and H_2 system, although the elastic momentum transfer cross-section shows a sharp drop as the energy approaches 1 eV (Figures 1 and 2), it is small and overshadowed by the much more intense proton transfer process. Therefore, in this system, there is no maximum observed in either bulk or flux reduced mobility (Figure 7), and these values monotonically decrease with increasing electric field. The bulk reduced mobility value is higher than the flux reduced mobility value, just as the bulk drift velocity is higher than the flux drift velocity.

In Figure 8, the bulk and flux values of longitudinal and transverse diffusion coefficients, multiplied by the gas concentration, are shown as a function of E/N. The bulk diffusion coefficient values are calculated as

$D_L^B = 0.5\Delta(\langle z^2 \rangle - \langle z \rangle^2)/\Delta t$,
$D_T^B = 0.25(\Delta\langle x^2 \rangle/\Delta t + \langle y^2 \rangle/\Delta t)$,

while the flux diffusion coefficient values are calculated as

$D_L^F = \langle v_z z \rangle - \langle v_z \rangle\langle z \rangle$,
$D_T^F = 0.5(\langle v_x x \rangle + \langle v_y y \rangle)$.

For $E/N < 100$ Td, the significantly lower D_L than D_T indicates highly anisotropic diffusion of the swarm, which spreads four times slower in the direction of the field, deforming the swarm's spherical shape into a highly ellipsoidal shape.

The reduction of diffusion coefficients with increasing E/N is attributed to the rising number of charge exchange reactions with energy that produce slow
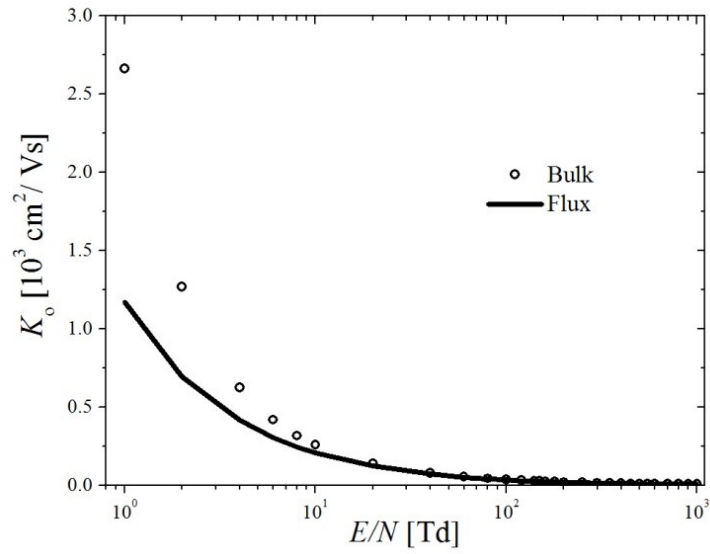
Figure 7. Bulk and flux reduced mobility for H_2^+ in H_2 a function of E/N at 300 K.
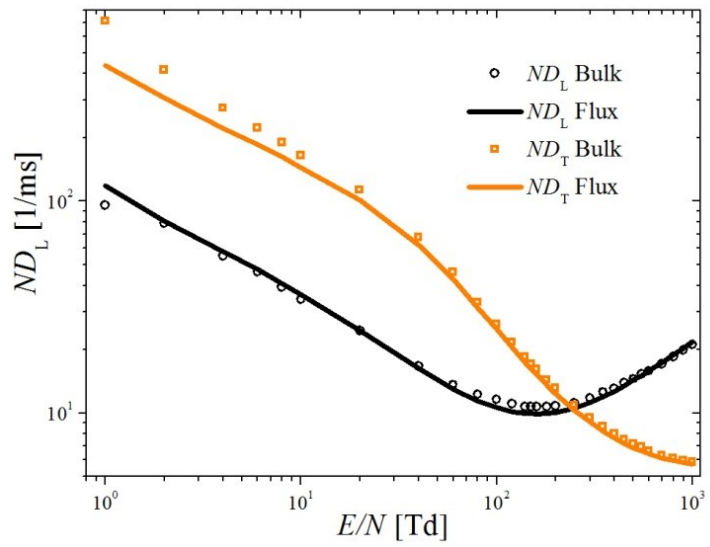

Figure 8. Bulk and flux longitudinal and transverse diffusion coefficients as a function of E/N at 300K.

H_2^+ ions. Consequently, as the electric field intensifies, the population of slow H_2^+ ions also increase (as depicted in Figures 2 and 3), significantly impeding longitudinal diffusion. While there are minor differences between the bulk and flux values of diffusion coefficients, as evident in Figure 8, except for transverse diffusion at low fields, where the bulk values surpass the flux values.

From Figure 9, it is evident that the rate coefficients for rotational and vibrational excitations (denoted in the figure as RE1, RE2, Vib1, Vib2, and Vib3) exhibit an upward trend as the electric field strength increases. This trend is attributed to the increased overlap between the Ion energy probability functions (depicted in Figure 3 and Figure 4) and the respective collision frequencies for excitations, which depend on the energy level.
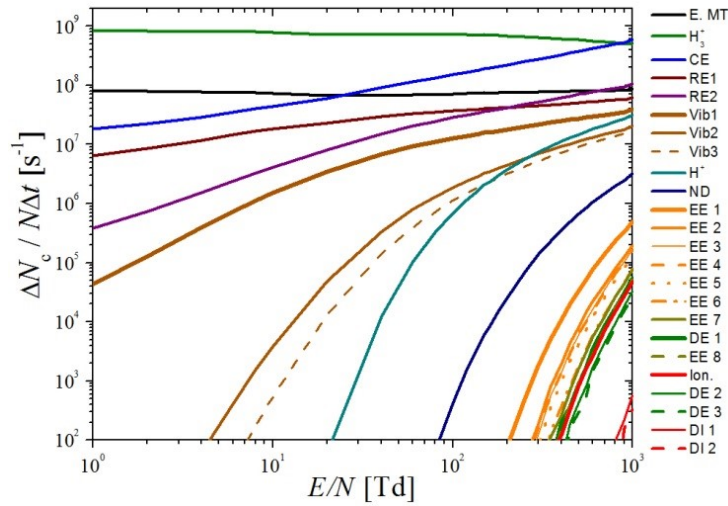

Figure 9. Rate coefficients for H_2^+ in H_2 a function of E/N at 300 K. The lines representing the rate coefficients correspond to the lines for the corresponding cross-sections shown in Figure 2.

4. Conclusion

In this paper we have determined the cross section of elastic moment transport as a function of energy for H_2^+ scattering on H_2 that can be used in modeling H_2^+ transport in H_2 gas. We used the data for a simple theoretical cross-section of the transmission of the total moment and obtained the cross-section of the transmission of the elastic moment by deduction of all experimentally obtained cross-sections of the charge exchange. In doing so, we assumed that the measured cross-sections of the charge exchange were collisions with the highest probability. Thus, in this paper, we have estimated the set of cross sections for H_2^+ ions in H_2

that can be used as an independent input in modeling H_2^+ ion transport. This estimation was performed using measured cross-sections of charge exchange.

Since, according to our knowledge, there is no direct information in the literature on how the mobility of high recombination energy ions, such as H_2^+ ions, behave in H_2 gas, we calculated transport parameters using the Monte Carlo simulation method (Nikitović *et al.*, 2014; Nikitović *et al.*, 2019).

In this work, we obtained and considered data on mean energy, drift velocity, longitudinal and transversal diffusion coefficients, bulk and flux reduced mobility and rate coefficients. Data on swarm coefficients for positive and negative ions are required for hybrid and fluid codes (White *et al.*, 2014; Marjanović *et al.*, 2016) and the current focus on liquids or liquids in rare gas mixtures dictates the need to produce data compatible with these models. Given the current interest in liquid and / or liquid models in mixtures with rare gases, data on swarm coefficients for positive and negative ions for hybrid and fluid codes are needed.

References

Denpoh K. and Nanbu K.: Comprehensive ion-molecule reactive collision model for processing plasmas, 2022, *Journal of Vacuum Science & Technology Å 40* **063007**, doi: 10.1116/6.0002098

Denpoh K. and Nanbu K.: Self-consistent particle simulation of radio-frequency CF_4 discharge with implementation of all ion–neutral reactive collisions, 1998, *J. Vac. Sci. Technol. A* **16**, 1201, DOI: doi.org/10.1116/1.581259

Fraga M.M.F.R., Fraga F.A.F., Fetal S.T.G., Margato L.M.S., Ferreira Marques R., Policarpo A.J.P.L.: The GEM scintillation in He–CF_4, Ar–CF_4, Ar–TEA and Xe–TEA mixtures, 2003, *Nucl. Instrum. Meth. in Phys. Res. A* **504**, 88, DOI: doi.org/10.1016/S0168-9002(03)00758-7

Golzar K., Amjad-Iranagh S., Amani M., Modarress H.: Molecular simulation study of penetrant gas transport properties into the pure and nanosized silica particles filled polysulfone membranes, 2014, *J. Membrane Science* **451**, 117 https://doi.org/10.1016/j.memsci.2013.09.056

Kaboth A., Monroe J., Ahlen S., Dujmić D., Henderson S., Kohse G., Lanza R., Lewandowska M., Roccaro A., Sciolla G., Skvorodnev N., Tomita H., Vanderspek R., Wellenstein H., Yamamoto R., Fisher P.: A measurement of photon production in electron avalanches in CF_4, 2008, *Nucl. Instrum. Meth. in Phys. Res. A* **592**, 63, DOI: doi.org/10.1016/j.nima.2008.03.120

Krstić P. S. and Schultz D. R.: Elastic and related transport cross sections for singly charged ion–atom scattering of light metals (Li, Be, B) and hydrogen, 2009, *J. Phys. B: At. Mol. Opt. Phys.* **42**, 065207
DOI 10.1088/0953-4075/42/6/065207

Mason E.: Scattering of Low-Velocity Molecular Beams in Gases, 1957, *J. Chem. Phys.* **27**, 782
https://doi.org/10.1063/1.1743829

Marjanović S., Banković, D. Cassidy A., Cooper B., Deller A., Dujko S. and Petrović Z. Lj.: A CF4 based positron trap, 2016, *J. Phys. B: At. Mol. Opt. Phys.* **49**, 215001
10.1088/0953-4075/49/21/215001

Ness K. F. and Robson R. E.: Velocity distribution function and transport coefficients of electron swarms in gases. II. Moment equations and applications, 1986, *Phys. Rev. A* **34**, 2185, DOI: doi.org/10.1103/PhysRevA.34.2185

Nikitović Ž., Raspopović Z. and Stojanović V.: Cross sections set and transport coefficients for Ar^+ in Ar/CF_4 mixtures, 2018, *Eur. Phys. J. D* **72**, 168, DOI: doi.org/10.1140/epjd/e2018-90059-1

Nikitović Ž., Raspopović Z.: Rate coefficients for Ar^+ in Ar/BF_3 mixtures, 2021, *Eur. Phys. J. D* **75**, 118, DOI:10.1140/epjd/s10053-021-00061-3

Nikitović Ž., Raspopović Z., Stojanović V. and Jovanović J.: Transport parameters of F-ions in Ar/BF_3 mixtures, 2014, *EPL* **108**, 35004, DOI:10.1209/0295-5075/108/35004

Nikitović Ž. D., Stojanović V. D. and Raspopović Z. M.: Modeling elastic momentum transfer cross-sections from mobility data, 2016, *EPL* **114**, 25001, DOI:10.1209/0295-5075/114/25001

Nikitović Ž., Raspopović Z. and Stojanović V.: Reduced mobility of Ar^+ in Ar/BF_3 mixtures, 2019, *EPL* **128**, 15001, DOI:10.1209/0295-5075/128/15001

Petrović Z. Lj., Raspopović Z. M., Stojanović V. D., Jovanović J. V., Malović G., Makabe T. and de Urquijo J.: Data and modeling of negative ion transport in gases of interest for production of integrated circuits and nanotechnologies, 2007, *J. Appl. Surf. Sci.* **253**, 6619
https://doi.org/10.1016/j.apsusc.2007.02.005

Phelps A. V.: Cross Sections and Swarm Coefficients for H^+, H_2^+, H_3^+, H, H_2, and H_- in H_2 for Energies from 0.1 eV to 10 keV, 1990, *J. Phys. Chem. Ref. Data* **19**, 653
doi.org/10.1063/1.555858

Phelps A. V.: Energetic ion, atom, and molecule reactions and excitation in low-current H_2 discharges:Model 2009, *Phys. Rev. E* **79**, 066401
https://doi.org/10.1103/PhysRevE.79.066401

Phelps A. V.: Collisional kinetics of non-uniform electric field, low-pressure, direct-current discharges in H_2, 2011, *Plasma Sources Sci. Technol.* **20**, 043001
DOI 10.1088/0963-0252/20/4/043001

Ristivojević Z. and Petrović Z. Lj.: A Monte Carlo simulation of ion transport at finite temperatures, 2012, *Plasma Sources Sci. Technol.* **21**, 035001
DOI 10.1088/0963-0252/21/3/035001

Radzig A. A. and Smirnov B. M.: Reference Data on Atoms, Molecules, and Ions, (Springer, New York, 1985), *p. 444* **ISBN 10: 3540124152**, ISBN 13: 9783540124153

Robson R. E., White R. D., Petrovic Z. Lj.: Colloquium: Physically based fluid modeling of collisionally dominated low-temperature plasmas, 2005, *Rev. Mod. Phys.* **77**, 1303, DOI:10.1103/RevModPhys.77.1303

Todd B., Young J. B.: Thermodynamic and transport properties of gases for use in solid oxide fuel cell modelling, 2002, *J. Power Sources* **110**, 186 https://doi.org/10.1016/S0378-7753(02)00277-X

White R. D., Tattersall W., Boyle G., Robson R. E., Dujko S., Petrović Z. Lj., Banković A., Brunger M. J., Sullivan J. P., Buckman S. J. and Garcia G.: Low-energy electron and positron transport in gases and soft-condensed systems of biological relevance, 2014, *Applied Radiation and Isotopes* **83**, 77, DOI: doi.org/10.1016/j.apradiso.2013.01.008